

## **$P_{13}$ Phase Shift in $K^+p$ Reactions and an Exotic Resonance $Z_1^*(1860)$**

Toshio HAYASHI<sup>†</sup> and Toshihiko HATTORI\*

*Department of Physics, Faculty of Education, University of Kagawa  
Takamatsu, Kagawa*

*\*Department of Physics, College of General Education  
University of Tokushima, Tokushima*

(Received June 14, 1975)

$P_{13}$  partial wave amplitude of  $K^+p$  elastic scattering is investigated from the information on the inelastic channels,  $K\Delta$  (1236) and  $K^*(891)p$  in terms of the three channel  $N/D$  model.

The calculated  $P_{13}$  phase shift shows a counterclockwise circle in the Argand diagram and has the maximum of phase shift versus energy at 1.15 GeV/ $c$  of kaon incident momentum. We argue that the exotic resonance  $Z_1^*$ , if it exists, is a highly inelastic resonance caused by the strong absorption through inelastic channels and is coupled very weakly with  $K^+p$  elastic channel.

### § 1. Introduction

Total cross section of  $K^+p$  scattering shows a bump structure at about 1.25 GeV/ $c$  of the  $K^+$  incident momentum.<sup>1)</sup> Recently a number of experiments and analyses have been done in order to investigate whether or not the bump structure is due to the existence of an exotic resonance  $Z_1^*(1860)$ .<sup>2)</sup> Among these analyses, some of the solutions describe the resonance-like behavior in the Argand diagram of the  $P_{13}$  wave and suggest the possible existence of  $Z_1^*$ . However, there is no final conclusion of the exotic resonance problem because the phase shift analysis based on the data on the  $K^+p$  elastic differential cross section and polarization have not presented a unique solution, but have allowed several solutions on account of no measurement of spin rotation parameters. All experiments which show some resonance features share the common characteristics, i.e., the  $K^+p$  elastic  $P_{13}$  wave is very inelastic and the speed of the Argand circle (the rate of change of the phase shift with energy) gives broad peak or almost flat structure versus energy.<sup>3)</sup> These facts mean that the resonance, if it exists, is coupled very weakly with the  $K^+p$  elastic channel. Therefore, we conclude that the conventional phase shift analysis of single energy type based on the shortest path criterion is rather insensitive to the decision as to whether  $Z_1^*$  resonance exists or not.<sup>4),5)</sup>

Bland et al. performed an experiment on single-pion production of the  $K^+p$

<sup>†</sup> Present address: Department of Physics, College of General Education, Osaka University, Toyonaka, Osaka.

system and tried the partial wave analysis of the  $K\Delta(1236)$  and  $K^*(891)p$  production amplitudes in the uncoupled channel treatment.<sup>6)</sup> They concluded that the total cross section peak at about 1.25 GeV/c does not represent the existence of the substantial resonance component in any partial wave amplitudes of  $K\Delta$  production, but the bump arises from the superposition of the  $K\Delta$  and  $K^*p$  channel cross sections which are smooth but have widely separated thresholds. That is to say, they interpreted the bump of total cross section as a threshold effect resulting from the sharp raises of  $\Delta$  and  $K^*$  production cross sections.

Therefore, it is significant to perform a coupled-channel partial wave analysis of the  $K^+p$  system by taking account of inelastic processes,  $K^+p \rightarrow K\Delta(1236)$  and  $K^+p \rightarrow K^*(891)p$ . If we reproduce the experiment of both elastic and inelastic channels in terms of the multi-channel approach, we can reduce several phase shift solutions to a unique one and we will be able to make clear the mechanism of the  $K^+p$  system.

We perform the analysis of the  $K^+p$  elastic  $P_{13}$  wave in the range of momentum from 0.8 GeV/c to 1.6 GeV/c. It is interesting and important for the following three reasons to investigate the elastic  $P_{13}$  wave: The first reason is the possible existence of  $Z_1^*$  resonance. In terms of simple quark model we cannot construct  $Z_1^*$  from three quarks. If  $Z_1^*$  does not exist in the  $K^+p$  elastic channel, Regge poles must be exactly exchange degenerate in the crossed channel. The second reason is the structure of the absorption coefficient in  $K^+p$  elastic scattering. Usually the absorption coefficient shows the central absorption with Gaussian type at high energies in terms of the impact parameter representation.<sup>7)</sup> This behavior is considered to represent the characteristic feature of Pomeron. But at low energies, the behavior of absorption coefficient is peripheral.<sup>8)</sup> Among partial waves of  $K^+p$  elastic scattering amplitudes,  $P_{13}$  wave is most absorbed and its coefficient plays an important role in the peripheral behavior. If we suppose that the phase shift of Pomeron is purely imaginary and its  $S$ -matrix is equal to the absorption coefficient, we may clarify the content of Pomeron at low energies by the investigation of the absorption coefficient with this peripheral character.<sup>8)</sup> The last reason is that the  $K^+p$  system has many features common to the proton-proton system at low energies. Both systems have an exotic resonance problem. The  $p$ - $p$  elastic scattering channel is also an exotic process in  $s$ -channel but with baryon number equal to two and has the possible existence of di-proton resonance in the elastic  $^1D_2$  wave.<sup>9)</sup> The absorption coefficient also behaves peripherally.<sup>10)</sup>

Now, we discuss the dominance of the  $P_{13}$  wave in the two inelastic channels,  $K^+p \rightarrow K\Delta$  and  $K^+p \rightarrow K^*p$ . According to the partial wave analyses of  $K\Delta$  production angular distribution, the  $P_{13}$  wave contributes largely in the low energy region near threshold.<sup>4), 6)</sup> The analysis of  $K^*p$  production by Bland et al. tells us that the  $P_{13}$  wave is also large near the threshold. But the detailed analysis of  $K^*p$  production is insufficient on account of poor data on the  $K^*p$  angular distribution.

One of the present authors (T. H.) has performed the partial wave analysis of the Regge amplitudes which reproduce the experiment of differential cross sections and the inelastic total cross sections of  $K\Delta$  and  $K^*p$  productions at low energies.<sup>11)</sup> He has obtained the result that the  $P_{13}$  wave contributes most largely to both reactions at  $P_{\text{lab}} < 1.6 \text{ GeV}/c$ . The analysis in terms of one-boson exchange amplitudes (OBE model) has given the same result at least in the momentum range  $P_{\text{lab}} < 1.2 \text{ GeV}/c$ .<sup>12)</sup> Then, we may conclude that there is a large  $P_{13}$  wave contribution at the raises of these production cross sections and we expect that the  $K^+p$  elastic  $P_{13}$  state is coupled with  $K\Delta$  inelastic  ${}^2P_{13}$  state and  $K^*p$  inelastic  ${}^2P_{13}$  and  ${}^4P_{13}$  states strongly.

In this paper we will investigate the  $K^+p$  elastic  $P_{13}$  wave in terms of three-channel model coupled with the inelastic reactions  $K^+p \rightarrow K\Delta$  and  $K^+p \rightarrow K^*p$ , on the basis of the coupled  $N/D$  equations. In our analysis it is assumed that the  $P_{13}$  wave is completely dominated in these quasi-two-body final states over the momentum range from the thresholds to the first peaks of these production cross sections. Further it is assumed that the  $N$  function in the  $N/D$  equations which represents the left-hand cut singularity can be phenomenologically approximated in terms of one-pole term. The pole position  $T_1$  and residue  $a_{ij}$  are regarded as adjustable parameters to reproduce the experiment of inelastic cross sections  $\sigma(K^+p \rightarrow K\Delta)$  and  $\sigma(K^+p \rightarrow K^*p)$ . Then, it is possible to study the  $P_{13}$  wave phase shift and absorption coefficient in the  $K^+p$  elastic channel by the use of these adjusted parameters. In § 2, we outline the formalism of the coupled channel  $N/D$  model. In § 3, the calculation is performed and the results are compared with data. The last section is devoted to conclusions and discussion.

## § 2. Coupled channel $N/D$ formalism for $K^+p$ scattering

In this section we start with a coupled channel  $N/D$  representation for the  $K^+p$  scattering amplitude  $\mathbf{M}$ . For simplicity, it is assumed that there is no C.D.D. pole and no anomalous singularity in the  $N/D$  equations. It is, moreover, assumed that the left-hand cut integral which represents a force in the  $K^+p$  system can be approximated by one-pole term. Then, we obtain the following equations:

$$M_{ij} = \rho_i^{1/2} (\mathbf{N}\mathbf{D}^{-1})_{ij} \rho_j^{1/2}, \quad (2.1)$$

$$N_{ij}(T) = \frac{a_{ij}}{T - T_1}, \quad (2.2)$$

$$D_{ij}(T) = \delta_{ij} - \frac{T - T_1}{\pi} \int_{T_i^{\text{th}}}^{\infty} \frac{\rho_i(T') N_{ij}(T')}{(T' - T)(T' - T_1)} dT', \quad (2.3)$$

where the subscript  $i$  (or  $j$ ) = 1, 2, 3 refer to the channels  $K^+p$ ,  $K\Delta$  and  $K^*p$  respectively.  $T$  is the laboratory kinetic energy of incident kaon,  $T_1$  denotes the pole position and the pole residue  $a_{ij}$  denotes an element of real symmetric (3, 3)

matrix. The *D* function is normalized to **1** at  $T=T_1$ .  $T_i^{\text{th}}$  is the ordinary unitary threshold energy of the *i*-th channel.  $\rho_i(T)$  appearing in Eq. (2.3) is a phase space factor of the *i*-th channel and is defined from the threshold behavior as follows:

$$\rho_1(T) \equiv \frac{q_{1,\text{c.m.}}^3}{\sqrt{s}} = \frac{[(T+m)^2 - m^2]^{3/2}}{[(1+m)^2 + 2T]^2}, \quad (2.4)$$

$$\rho_2(T) = \frac{1}{W} \int_{1+\mu}^{\sqrt{s}-m} \frac{dM'}{(M'-M^*)^2 + (\Gamma/2)^2} \rho_2(M', T) \quad (2.5)$$

with

$$\rho_2(M', T) \equiv \frac{q_{2,\text{c.m.}}^3}{\sqrt{s}} = \frac{[(1+2m+2T-M'^2)^2 - (2mM')^2]^{3/2}}{[(1+m)^2 + 2T]^2} \quad (2.6)$$

and

$$W \equiv \int_{1+\mu}^{\infty} \frac{dM'}{(M'-M^*)^2 + (\Gamma/2)^2}. \quad (2.7)$$

Here masses are expressed in nucleon mass units (938 MeV),  $q_{i,\text{c.m.}}$  represents the c.m. momentum of *i*-th channel,  $\sqrt{s}$  the c.m. total energy,  $\mu$  the pion mass,  $m$  the kaon mass;  $M^*$  and  $\Gamma$  (116 MeV) denote the mass and width of  $\Delta(1236)$ , respectively.  $\rho_2(T)$  is averaged by the Breit-Wigner mass spectrum of  $\Delta$  mass. The expression for  $\rho_3(T)$  is similar to  $\rho_2(T)$ :  $\rho_3(T)$  is obtained by replacing the mass and width of  $\Delta$  in  $\rho_2(T)$  by the mass and width (=50 MeV) of  $K^*(891)$  respectively also in nucleon mass units. Since  $\rho_i(T)$  ( $i=1, 2$  or  $3$ ) becomes linear in  $T$  as  $T \rightarrow \infty$ , the dispersion integral of Eq. (2.3) converges under the one-pole approximation of the *N* function.

We substitute Eq. (2.2) into the *D* function of Eq. (2.3) and define the following function  $f_i(T)$ :

$$D_{ij}(T) = \delta_{ij} + a_{ij}f_i(T) \quad (2.8)$$

with

$$f_i(T) = -\frac{T-T_1}{\pi} \int_{T_i^{\text{th}}}^{\infty} \frac{\rho_i(T')}{(T'-T)(T'-T_1)} dT'. \quad (2.9)$$

If we substitute the concrete expressions for  $\rho_i(T)$  of Eqs. (2.4)~(2.7) into Eq. (2.9) and exchange the order of integrals in these equations for  $i=2$ , we obtain the following expressions:

$$f_1(T) = -\frac{T-T_1}{\pi} \int_0^{\infty} \frac{[(T'+m)^2 - m^2]^{3/2}}{[(1+m)^2 + 2T']^2 (T'-T)(T'-T_1)} dT', \quad (2.10)$$

$$f_2(T) = \frac{1}{W} \int_{1+\mu}^{\infty} \frac{dM'}{(M'-M^*)^2 + (\Gamma/2)^2} f_2(M', T) \quad (2.11)$$

with

$$f_2(M', T) \equiv -\frac{T-T_1}{\pi} \int_{T_0}^{\infty} \frac{[(1+2m+2T'-M'^2)^2 - (2mM')^2]^{3/2}}{[(1+m)^2 + 2T']^2 (T'-T)(T'-T_1)^2} dT' \quad (2.12)$$

and

$$T_0 = \frac{1}{2} [(M' + m)^2 - (1 + m)^2] \geq (1 + m)\mu + \frac{1}{2}\mu^2 \equiv T_2^{\text{th}}. \quad (2.13)$$

The expressions for  $f_3(T)$  and  $f_3(M', T)$  are obtained by the same replacement of  $f_2(T)$  and  $f_2(M', T)$  respectively as mentioned already below Eq. (2.7). The above expressions for  $f_1(T)$ ,  $f_2(M', T)$  and  $f_3(M', T)$  can be integrated analytically. Therefore, we can evaluate  $f_2(T)$  and  $f_3(T)$  numerically if the value of pole position  $T_1$  is given as a parameter.

Accordingly, if the parameters  $T_1$  and  $a_{ij}$  are given, we can calculate the partial wave amplitudes of elastic scattering and  $K\mathcal{A}$  and  $K^*p$  productions. Then, these parameters must be adjusted to reproduce the data.

The phase shift parameters  $(\delta, \eta)$  of  $K^+p$  elastic  $P_{13}$  wave can be extracted from the scattering amplitude through

$$M_{11} \equiv \frac{1}{2i} (\eta e^{2i\delta} - 1) = \rho_1(T) (\mathbf{ND}^{-1})_{11}. \quad (2.14)$$

The partial cross sections of  $K^+p$  elastic scattering and  $K\mathcal{A}$  and  $K^*p$  productions are expressed as follows:

$$\sigma^{\text{el}}(P_{13}) = \frac{8\pi}{q_1^2} \rho_1^2(T) |(\mathbf{ND}^{-1})_{11}|^2. \quad (2.15)$$

$$\sigma^{K\mathcal{A}}(^4P_{13}) = \frac{8\pi}{q_1^2} \rho_1(T) \rho_2(T) |(\mathbf{ND}^{-1})_{21}|^2, \quad (2.16)$$

$$\sigma^{K^*p}(^4, ^2P_{13}) = \frac{8\pi}{q_1^2} \rho_1(T) \rho_3(T) |(\mathbf{ND}^{-1})_{31}|^2. \quad (2.17)$$

### § 3. Calculations and comparison with data

As an input information which derives the phase shift parameters  $(\delta, \eta)$  of  $K^+p$  elastic  $P_{13}$  partial wave we may employ the production cross sections  $\sigma(K\mathcal{A})$  and  $\sigma(K^*p)$ . In our treatment of  $K\mathcal{A}$  production data, we use the  $K^0\mathcal{A}^{++}$  cross section multiplied by 4/3 in order to include all of  $K\mathcal{A}$  charged states. It is assumed that each of the cross sections  $\sigma(K\mathcal{A})$  and  $\sigma(K^*p)$  is dominated by the transitions,  $K^+p(^2P_{13}) \rightarrow K\mathcal{A}(^4P_{13})$  and  $K^+p \rightarrow K^*p(^4P_{13}$  and  $^2P_{13})$  respectively. As we have already investigated in § 1, this assumption is accepted experimentally in the momentum range from thresholds to 1.2 GeV/ $c$  for  $\sigma(K\mathcal{A})$  and also to 1.6 GeV/ $c$  for  $\sigma(K^*p)$ . In the regions above these energies the contribution of  $P_{13}$  wave does not dominate and should be properly smaller than the experimental values of  $K\mathcal{A}$  and  $K^*p$  production cross sections. Then, we make use of the data of  $\sigma(K\mathcal{A})$  at 1.367,

1.450, 1.560 and 1.585 GeV/c and the data of  $\sigma(K^*p)$  at 1.960 GeV/c as upper bounds to reproduce the bump structures of these production cross sections.

We perform a  $\chi^2$ -minimization about the pole position  $T_1$  and the pole residue  $a_{ij}$  as adjustable parameters. The value of  $T_1$  is varied in the range between  $-1400$  MeV/c and  $-100$  MeV/c in which  $\rho$ -meson exchange cut ( $-935$  MeV/c to  $-364$  MeV/c) is covered. The reason is that the most nearby singularities of  $K^+p \rightarrow K^+p$  and  $K^+p \rightarrow K\Delta$  reactions are expected to be brought about by  $\rho$ -meson exchange. There are the following ambiguities corresponding to the arbitrariness of the relative phase in the state vectors,

$$(a_{12}, a_{13}, a_{23}) \leftrightarrow (-a_{12}, -a_{13}, a_{23}) \leftrightarrow (-a_{12}, a_{13}, -a_{23}) \leftrightarrow (a_{12}, -a_{13}, -a_{23}).$$

We choose the phase so that the values of  $a_{12}$  and  $a_{13}$  become positive or zero.

After the  $\chi^2$ -minimization, we have obtained three solutions which have similar features with the exception of a slight difference of the production cross sections in the energy regions above the bumps. On account of the assumption that the  $P_{13}$  wave dominates only in the energy range from thresholds to the first peaks and does not dominate above the energy regions, we choose the solution which gives a smaller value of the cross sections in the energy regions above the bumps. The value of  $\chi^2$  of the solution is equal to 3.92. In Fig. 1, the calculated values are compared with the data on the production cross sections.<sup>13)</sup> The values of adjusted parameters  $T_1$  and  $a_{ij}$  are given in Table I. As seen in Fig. 1, the coupled channel  $N/D$  model with the parameters in Table I reproduces the experimental data with the sharp raises at the thresholds and the bump structures. In Fig. 2, the phase shift and absorption coefficient of  $K^+p$  elastic scattering are shown.

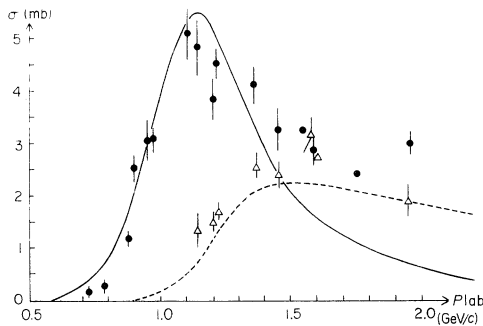


Fig. 1. The cross sections  $\sigma(K^+p \rightarrow \text{all } K\Delta)$  and  $\sigma(K^+p \rightarrow K^*p)$   $\bullet$ : all  $K\Delta$  production cross section data and  $\triangle$ :  $K^*p$  production cross section data. Solid and dotted curves are the predictions of all  $K\Delta$  and  $K^*p$  production cross sections respectively with the adjusted parameters in Table I.

Our result is compared with the solutions of phase shift analysis in the momentum range below 730 MeV/c in Fig. 2(a).<sup>14)</sup> We see that our result can be considered to be in agreement with this solution at low energies below the  $K\Delta$  threshold. As seen in Fig. 2(a), the phase shift has a

Table I. Values of parameters  $T_1$  and  $a_{ij}$ .  $\chi^2=3.92$ .

$T_1$ (MeV)	$a_{11}$	$a_{12}$	$a_{13}$	$a_{22}$	$a_{23}$	$a_{33}$
-411.1	-7.960	10.99	9.249	-7.105	-9.181	-7.863

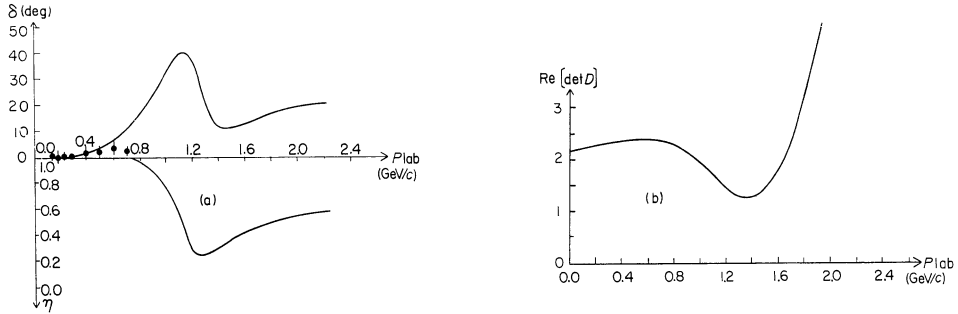


Fig. 2(a):  $K^+$  incident momentum dependence of the phase shift and the absorption coefficient of  $K^+p$  elastic  $P_{13}$  partial wave. (b): The real part of  $\det \mathbf{D}$   $\text{Re}(\det \mathbf{D})$ . •: The results of the  $K^+p$  elastic  $P_{13}$  phase shift analysis.<sup>14)</sup>

characteristic energy dependence; a sharp bump peaked at 1.15 GeV/c and associated with a broad dip. This structure can be explained as an absorption effect caused by the inelastic channels.<sup>15)</sup> As shown in Fig. 2(b), the real part of the determinant of  $D$  function matrix  $\text{Re}(\det \mathbf{D})$  has a dip at  $P_{lab}=1.35$  GeV/c. We can infer from this fact that the resonance zero is able to appear on the second Riemann sheet. As seen in Fig. 3, the Argand diagram and the speed of  $K^+p$  elastic  $P_{13}$  wave show the resonance-like behavior and the mass of resonance is estimated to be 1860 MeV. This behavior is qualitatively consistent with the solutions of the phase shift analyses by the CERN group<sup>16)</sup> and the ANL group.<sup>17)</sup> All the diagonal elements of adjusted parameters  $a_{ij}$  are negative as seen in Table I. This fact means that the force of each elastic channel is repulsive. Nevertheless, the phase shift is positive and behaves like a resonance. The reason is that the off-diagonal elements of  $a_{ij}$  are comparable with or slightly larger than the diagonal elements, so that the  $K^+p$  elastic channel is coupled strongly with  $K\Delta$  and  $K^*p$  inelastic channels.



Fig. 3(a): The Argand loop of  $P_{13}$  wave. The marked points are  $K^+$  incident momentum. (b): The speed of the Argand loop.

#### § 4. Concluding remarks

We have obtained the  $K^+p$  elastic  $P_{13}$  wave from the information on the  $K\Delta$  and  $K^*p$  production channels in terms of the three-channel  $N/D$  method. The results are summarized as follows: (1) The one-pole approximation which stands for a force in the  $K^+p$  system is a good approximation to reproduce the experiment

of these inelastic channels; (2) the phase shift of  $K^+p$  elastic  $P_{13}$  wave shows the characteristic features, i.e., the sharp bump and the associated broad dip, which are caused by the strong absorption effect of the inelastic  $K\Delta$  and  $K^*p$  channels; (3) the resonance-like behavior appears with the mass 1860 MeV; (4) similar features are found in  ${}^1D_2$  state of  $p$ - $p$  elastic scattering.<sup>9)</sup>

As already investigated in § 3, the assumption that the  $P_{13}$  wave dominates in  $K\Delta$  production is natural in our model and is consistent with the analysis by Bland et al. The model also reproduces the  $K^*p$  production data. However, the assumption of the  $P_{13}$  wave dominance in the  $K^*p$  channel is not necessarily reliable on account of insufficient data on the  $K^*p$  production near the threshold. In order to investigate our model in more detail and to confirm the possible existence of  $Z_1^*$  resonance, we need more experimental data on the production reactions of  $K^+p$  system. Especially, we need the angular distribution data and the partial wave analysis of the  $K^*p$  production.

We will say that, even if  $Z_1^*$  resonance exists experimentally, it is highly inelastic resonance caused by the strong absorption through inelastic channels and the resonance is coupled very weakly with the  $K^+p$  elastic channel. This fact means that (1) the main decay mode of resonance is expected to be the  $K\Delta$  channel from the analysis of Griffiths et al. in which  ${}^4P_{13}$  wave describes a counterclockwise loop in the Argand diagram,<sup>4)</sup> (2) there is no contradiction to selection rules forbidding the couplings of  $Z_1^*$  with normal strength to  $K^+p$  elastic channel, as suggested by multiquark model incorporating exotic resonances<sup>18)</sup> and (3) Regge poles of the crossed channel of  $K^+p$  elastic scattering should be approximately exchange degenerate.

### Acknowledgements

The authors would like to express their gratitude to Dr. M. Bando and Mr. Y. Aihara, Kyoto University for their valuable discussions and continual encouragement. One of the authors (T. H.) expresses his cordial thanks to Prof. S. Furuichi and Dr. H. Suzuki, Rikkyo University for their discussions.

Numerical calculations were performed at the Computer Center of Kagawa University with TOSBAC-3400 and at the Data Processing Center, Kyoto University with FACOM 230-60.

### References

- 1) R. L. Cool et al., Phys. Rev. Letters **17** (1966), 102.
- 2) For a review of the status of  $K^+p$  phase shift analysis and references, see V. Chaloupka et al., Phys. Letters **50B** (1974), 147.
- 3) S. C. Loken et al., Phys. Rev. **D6** (1972), 2346.
- 4) F. Griffiths et al., Nucl. Phys. **B38** (1972), 365.
- 5) R. A. Arndt et al., Phys. Rev. Letters **33** (1974), 987.
- 6) R. W. Bland et al., Nucl. Phys. **B18** (1970), 537.



- 7) Y. Higuchi and S. Machida, *Prog. Theor. Phys.* **36** (1966), 313.
- 8) T. Hattori, *Genshikaku Kenkyu* (Circular in Japanese) **17** (1972), 701.
- 9) R. A. Arndt, *Phys. Rev.* **165** (1968), 1834.  
H. Suzuki, *Prog. Theor. Phys.* **50** (1973), 1080; **54** (1975), 143.
- 10) N. Hoshizaki, *Prog. Theor. Phys. Suppl. No. 42* (1968), 1.
- 11) T. Hattori, *Soryusiron Kenkyu* (mimeographed circular in Japanese) Vol. **49** (1974), A47.
- 12) T. Hattori and Y. Aihara, *J. Sci. Tokushima Univ.* **8** (1975), 17.
- 13) E. Bracci et al., "Compilation of Cross Sections II— $K^-$  and  $K^+$  Induced Reactions", CERN/HERA 72-2 (1972).
- 14) W. Cameron et al., *Nucl. Phys.* **B78** (1974), 93.
- 15) S. Furuichi and H. Suzuki, *Prog. Theor. Phys.* **39** (1968), 420.
- 16) M. G. Albrow et al., *Nucl. Phys.* **B30** (1971), 273.
- 17) R. C. Miller et al., *Nucl. Phys.* **B37** (1972), 401.
- 18) S. Kato et al., *Phys. Rev. Letters* **24** (1970), 615.